Medical Image Analysis 12 (2008) 535–545

Contents lists available at ScienceDirect

Medical Image Analysis

journal homepage: www.elsevier.com/locate/media

Robotic assistance for ultrasound-guided prostate brachytherapy

Gabor Fichtinger [a,b,*], Jonathan P. Fiene [c], Christopher W. Kennedy [b], Gernot Kronreif [d], Iulian Iordachita [b], Danny Y. Song [b], Everette C. Burdette [e], Peter Kazanzides [b]

[a] Queen's University, 25 Union Street, #725 Goodwin Hall, Kingston, ON, Canada K7L 3N6
[b] The Johns Hopkins University, Baltimore, MD, USA
[c] University of Pennsylvania, Philadelphia, PA, USA
[d] PROFACTOR Research and Solutions GmbH, Seibersdorf, Austria
[e] Acoustic Medsystems Inc., Urbana–Champaign, IL, USA

ARTICLE INFO

Article history:
Received 3 February 2008
Received in revised form 15 May 2008
Accepted 10 June 2008
Available online 18 June 2008

Keywords:
Medical robotics
Image guided surgery
Prostate cancer
Brachytherapy

ABSTRACT

We present a robotically assisted prostate brachytherapy system and test results in training phantoms and Phase-I clinical trials. The system consists of a transrectal ultrasound (TRUS) and a spatially co-registered robot, fully integrated with an FDA-approved commercial treatment planning system. The salient feature of the system is a small parallel robot affixed to the mounting posts of the template. The robot replaces the template interchangeably, using the same coordinate system. Established clinical hardware, workflow and calibration remain intact. In all phantom experiments, we recorded the first insertion attempt without adjustment. All clinically relevant locations in the prostate were reached. Non-parallel needle trajectories were achieved. The pre-insertion transverse and rotational errors (measured with a Polaris optical tracker relative to the template's coordinate frame) were 0.25 mm (STD = 0.17 mm) and 0.75° (STD = 0.37°). In phantoms, needle tip placement errors measured in TRUS were 1.04 mm (STD = 0.50 mm). A Phase-I clinical feasibility and safety trial has been successfully completed with the system. We encountered needle tip positioning errors of a magnitude greater than 4 mm in only 2 of 179 robotically guided needles, in contrast to manual template guidance where errors of this magnitude are much more common. Further clinical trials are necessary to determine whether the apparent benefits of the robotic assistant will lead to improvements in clinical efficacy and outcomes.

1. Introduction and background

Prostate cancer continues to be the second most common cancer in American men, with an estimated 225,000 new cases per year (Jemal et al., 2006). Low dose rate permanent prostate brachytherapy or shortly brachytherapy in this paper, entails permanent implantation of radioactive pellets, a.k.a. seeds, into the prostate to kill the cancer with radiation from inside out. The seeds are the size of a rice grain. The seeds are implanted at a density of about 1.4–1.6 seeds/cm^3 in a complex non-uniform pattern, by needles inserted across the perineum under transrectal ultrasound (TRUS) guidance (Wallner et al., 2001). Brachytherapy, in addition to surgical removal of the prostate and external beam radiation therapy, has emerged as a definitive treatment option for patients with early stage prostate cancer; a group representing the majority of new cases diagnosed nowadays. Brachytherapy is performed for at least 45,000 patients in the US every year and the number of procedures has been steadily rising (Cooperberg et al., 2004).

The long-term disease-free survival after brachytherapy is well above 90% when performed by leading brachytherapy specialists, but in the hands of average practitioners in community care settings it has been significantly less successful (Wei et al., 2002; Merrick et al., 2007). Merrick et al. reported from 2833 cases by 57 brachytherapists that over 37% of implants were inadequate, in terms of incomplete target coverage or excessively high dose levels, despite the exclusion of each brachytherapist's initial 20 patients. Quite surprisingly, no trend toward improvement within the first 100 patients per physician was seen. Faulty needle and source placement often cause insufficient dose to the cancer and/or inadvertent radiation of the rectum, urethra and bladder. The former causes failure of treatment, while the latter results in adverse side effects like rectal ulceration, incontinence and dysuria (painful urination). Increased dose to normal structures is well correlated with increased toxicity after brachytherapy, and despite the adoption of modern techniques, toxicity remains significant; urinary Grade 2 toxicity of 46% at 6 months and 23% at 12 months was reported by Zelefsky et al. (2000). Although rectal toxicity is generally considered to be moderate relative to other radiotherapy

* Corresponding author. Address: Queen's University, 25 Union Street, #725 Goodwin Hall, Kingston, ON, Canada K7L 3N6. Tel.: +1 613 539 8721; fax: +1 410 516 5553.
E-mail address: gabor@cs.queensu.ca (G. Fichtinger).

1361-8415/$ - see front matter © 2008 Elsevier B.V. All rights reserved.
doi:10.1016/j.media.2008.06.002

options, in patients pooled from two randomized trials, rectal bleeding was reported in $\geqslant$20% of patients, and 12% had some form of fecal incontinence (Merrick et al., 2003). A comparative cohort analysis of 1014 patients treated with brachytherapy, external beam, or radical prostatectomy revealed long-term health-related quality of life scores to be adversely affected in the urinary, bowel, and sexual domains for brachytherapy patients, and less favorable than for the other treatments (Wei et al., 2002). Furthermore, whereas most brachytherapy outcomes are reported with median follow-up times of 3–4 years (including that of Wei et al., 2002), Miller et al. (2005) noted that quality of life after brachytherapy continued to decline over time after four or more years, suggesting that most reports underestimate the true extent of morbidity. Clearly these reports underscore the need for advancements and for the widespread availability of such improvements.

It is universally accepted that increased accuracy in executing a precise implant plan should lead to good dosimetric outcome. At the same time, there are numerous technical difficulties in the procedure that make precise execution of the implant plan very difficult and often downright impossible. Typical causes include organ dislocation and deformation, tissue inhomogeneity, seed migration, intraoperative edema, instrumentation and calibration errors, needle deflection, and human errors. A large body of clinical research has been dedicated to these problems. The arsenal of currently known countermeasures was compiled by Wallner et al. (2001) in a definitive practical guide to clinical brachytherapy. Still, despite the strictest control over the intraoperative workflow, many implants fail and outcomes are rather unpredictable, particularly in community practice (Merrick et al., 2007).

In addition to continuing efforts to achieve accurate execution of a pre-made implant plan, intraoperative planning and dosimetry optimization have been receiving increasing attention (Zelefsky et al., 2003; Acher et al., 2006). These approaches, however, demand localization of the implanted needles and seeds during the procedure (Nag et al., 2001). If needles and seeds are localized in TRUS relative to the anatomy, the dose field can be analyzed and the remainder of the implant plan re-optimized. Needle positions can be rearranged to avoid overdosing and new seeds added to fill cold spots. Again, this function critically depends on our ability to track needles and seeds in real-time ultrasound images. There has been valuable research in this theme, for example, by the groups of Rohling and Salcudean (Harmat et al., 2006; Okazawa et al., 2006) and Fenster (Ding et al., 2006; Wei et al., 2006). Despite encouraging results and steady progress, clinically robust tracking and localization of the implanted seeds in TRUS is unavailable. One particular hindrance is that in all current brachytherapy systems, imaging actions and needle actions are decoupled as the needle and TRUS probe are both manually manipulated. Concurrent action with the needle and the TRUS probe requires four hands in the field: two hands to manipulate the needle and seeds and two extra hands to move the TRUS probe, while trying to predict the motion of the needle. First, there is no room for two people (or four hands) in the sterile field. Second, the process is coordinated by voice command with the medical physicist sitting at the treatment planning system (TPS) terminal, several meters away from the actual surgery. This clearly is a suboptimal scenario that demands definitive improvement.

Considering the problems mentioned above, a robotic assistant to manipulate the needle and TRUS probe simultaneously seems to be a logical alternative. In a fully integrated robotic system, TRUS and needle are spatially and temporally co-registered. This allows for optimal positioning of the TRUS probe while the needle is in motion and the seeds are being released from the needle. Thus, the near exact position of the needle and seed are *a priori* known relative to the TRUS image. In a confined search range we can more easily find their true positions in the TRUS image and update the effective dose field on the fly.

Robotic assistance offers additional advantages over conventional template guidance. The robot allows for continuum needle placement, while in conventional templates the guide holes are placed in a rectilinear grid of 5 mm resolution. Bi-directional needle angulation also offers manifold advantages over template guidance where all needles are forced to be parallel. Vertical needle slanting helps avoid pubic arch interference that happens when part of the prostate is hidden behind the pubic bone, disqualifying patients with large prostates (typically >55 cm^3) from brachytherapy (Wallner et al., 2001). Lateral angulation can assist in accounting for slight anatomical asymmetries, thereby potentially yielding more conformal dose. Other potential advantages of robotic assistant systems include improved needle insertion accuracy by reducing needle deflection and tissue deformation (Meltsner et al., 2007) and reduced procedure time. The latter is particularly important in reducing the likelihood of severe intraoperative edema. Another potential benefit may be reduced exposure of the operating crew to toxic dose by handling the sources remotely. To this end, Patriciu et al. (2007) demonstrated remotely actuated seed handling and insertion in training phantoms. This system was designed for use with MRI in a fetal patient position, with no apparent provision for its adaptation to standard clinical practice under TRUS guidance in lithotomy position. The costs and complexity of MRI-compatible mechatronics and instrumentation are also prohibitive. Finally, and perhaps most importantly, existing semi-automated seed guns like the popular Mick Applicator series already provide excellent implant speed and radiation safety, making it hard to justify full automation.

Several robotic systems have been proposed for TRUS-guided brachytherapy. Yu et al. (2007) proposed to actuate both the needle and the TRUS probe and completely replaced standard clinical equipment with their own. They tested individual modules of the prototype in phantoms. Phee et al. (2006) proposed to access the prostate through a single entry point on the perineum. They eliminated the translational motion of the needle in front of the perineum and used angulation only by 2-DOF remote center of motion kinematics implemented by goniometric arcs. Their concept resembled one of the earliest medical robots by Harris et al. (1997) used in transurethral resection of the prostate (TURP) for benign prostatic hyperplasia. (It is of particular historical note that this device was the first medical robot ever to remove tissue from a live human patient.) The aforementioned anatomical approach of Phee et al. (2006) is hampered by major problems. First, insertion of many needles through a single portal would certainly cause major morbidity, because the needles distributed in a cone would cut out a large amount of tissue from the perineal wall. Second, the lack of parallel needle trajectories results in suboptimal dose coverage. Finally, conical needle arrangement either yields an inhomogeneous dose field or demands radiation sources of variable activity, which is suboptimal in either case. In Phee et al. (2006), a much reduced design with manual actuation was demonstrated in a limited biopsy study. No complications were reported. They used a single needle entry portal, which would be clinically inadvisable for brachytherapy where the number of needle passes is much higher than in biopsy, typically 35 or more versus 6 or 8.

Fenster and colleagues have made major strides toward a more clinically feasible TRUS-guided robotic prostate brachytherapy system (Wei et al., 2004). They adopted an industrial serial-link robot for needle manipulation while motorizing a conventional TRUS probe to produce a smooth sagittal sweep in the rectum. They were the first to demonstrate synchronized needle and imaging action (in training phantoms) and their results on needle tracking and seed segmentation were particularly exquisite (Wan et al., 2005). Despite its many excellent qualifications, however, to our knowledge this system has not reached human trials. This in part had to do with the choice of the robot. Generally, it is rather difficult

to certify industrial serial-link arms for clinical use because their inherent safety is always drawn into question. Not insignificantly, the system needed elaborate calibration before each procedure because the needle manipulator robot and TRUS motion encoder were not mechanically coupled. Finally, and perhaps most importantly, the robotic assistant was not integrated with an existing and clinically certified treatment planning system. This forced the researchers to develop their own implant planning and optimization system, which is a major clinical engineering project by any measure. It takes several years to produce a smooth clinical-grade implant planning system that meets radiation safety standards and can receive ethics board clearance.

Our own first work in the subject was with a 3-DOF robotic device that provided 2-DOF remote center of motion and 1-DOF insertion, in lithotomy position (Fichtinger et al., 2002). Stereotactic registration between the robot and imager (we applied CT guidance) was exquisitely accurate and robust (Masamune et al., 2001). Overall, however, the system performed poorly in cadaver trials. The lack of Cartesian motion made path planning difficult and clinically insufficient in terms of dose coverage. (Actually, our system suffered from many of the same deficiencies as Phee et al. (2006) must have experienced several years later.) The friction transmission also slipped because fatty fluids accidentally lubricated the transmission, making needle insertion depth uncertain.

In more recent prior work, we adhered to clinical standards by using TRUS guidance in full lithotomy position (Fichtinger et al., 2006). We integrated a robotic assistant with an FDA-approved commercial TRUS-guided TPS (Interplant®, at the time developed by Burdette Medical Systems, Urbana–Champaign, IL) and thus demonstrated successful retrofitting of an existing conventional clinical system with a new robotic manipulator. We used a 6-DOF robot mounted on a bridge over the table. It had 3-DOF prismatic motion to move the needle to the insertion point, 2-DOF remote center of rotation motion to orient the needle, and 1-DOF translation to enter the needle to a predefined depth. The TRUS probe had translation and rotation inside the rectum with 2-DOF optoelectronic encoding, though still not actively moving. From a historical perspective, this was the first integration of a brachytherapy robot system with a complete commercial brachytherapy system, including the TPS, ultrasound unit, probe holder, stepper, floor stand, leg holder, and other attachments. While this was clearly a promising concept to pursue, the actual robot proved to be wholly inadequate for the task. The device was heavy, large, intrusive, and it collided with the C-arm fluoroscope during the procedure. (In standard practice, a mobile fluoroscope is positioned over the patient's abdomen to make qualitative observation of the implant several times during the procedure.) Calibration between the robot and TRUS was complicated and had to be repeated every time we adjusted the subject on the treatment table. In fact, it required two separate calibrations because there was an unencoded positioning arm between the Cartesian and rotation stages.

In this manuscript, we present a system freed from many shortcomings of our earlier prototypes. The primary contribution of this paper is the design and implementation of a small robotic manipulator that is compatible with standard equipment and workflow and fully integrated with an FDA-approved commercial TPS. Previously, we presented an abridged technical outline of this system in (Fichtinger et al., 2007). In this paper, we provide a much wider review of prior art, a more detailed description of the system, and results from a recent Phase-I clinical trial with a detailed discussion. We are giving the first report of a human trial in robotically assisted prostate brachytherapy.

The structure of the rest of the paper is as follows. In Section 2, we present the system design and implementation. Section 3 discusses the clinical workflow, Section 4 summarizes the results of phantom tests, Section 5 sums up the results of a pilot clinical trial, and we conclude the paper with an in-depth discussion of our findings.

2. System design and implementation

As reviewed in Section 1, several medical robots have been proposed previously for prostate brachytherapy. They all strive to increase the accuracy of needle placement by transforming the workflow into a process one could categorize, after Taylor, as "Surgical CAD/CAM" (Fichtinger et al., 2002). Unfortunately, these devices add a great deal of complexity to the procedure and alter current hardware, calibration, and workflow standards. Our present approach is different in that it adheres to the established standards of care, while also providing all practical benefits of robotic assistance.

The system consists of a central computer (laptop) running the FDA-approved Interplant® treatment planning system (TPS) originally developed by Burdette Medical and now manufactured by Computerized Medical Systems Inc., St. Louis, MO; a TRUS imager (B&K Medical, 6.5 MHz); an AccuSeed implant stand with digital probe positioner (also by Computerized Medical Systems); and a small parallel needle guidance robot, as shown in Fig. 1(left). We adapted a light weight parallel robot that rests on the mounting posts of the conventional template, as seen in Fig. 1(right). The robot and the template are interchangeable during the procedure, as they are mounted in the same location and are calibrated to

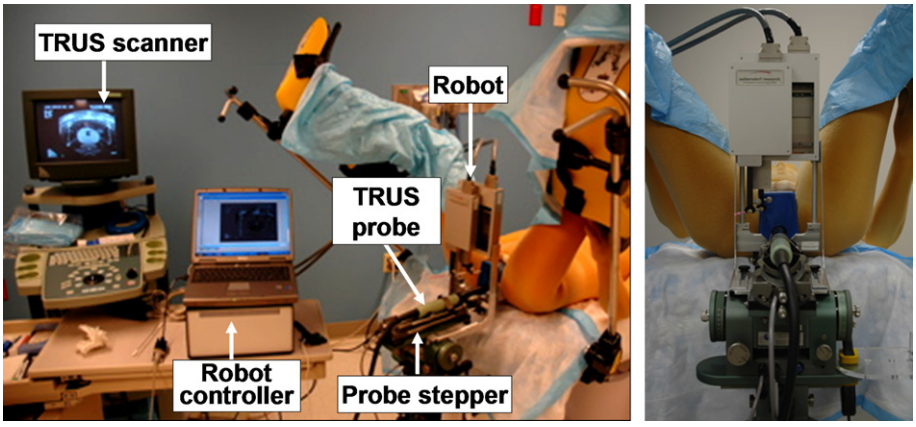

Fig. 1. System setup with an anthropomorphic phantom in the operating room (left) and a closer view of the robot from the physician's perspective (right). Note how the standard clinical hardware and setup are preserved.

operate in the same coordinate frame. Thus, the unique feature of our system is retaining the existing clinical setup, hardware and workflow. In the case of a malfunction or even a slight suspicion of it, the physician can revert to the conventional template-based manual procedure without interruption. The robot is controlled by a standalone computer, thereby preserving the integrity of the FDA-approved Interplant system. The TRUS unit and the encoded stepper produce temporally and spatially tagged image streams for the TPS. In the laboratory experiments reported in this paper, an anthropomorphic mannequin was positioned supine, with a standard brachytherapy implant training phantom (CIRS Inc., Norfolk, VA) built into its perineum, as shown in close-ups later in the pictures of Fig. 5.

The robot was originally developed for image-guided needle biopsy (Kettenbach et al., 2005) and was customized by the manufacturer (PROFACTOR GmbH, Seibersdorf, Austria) to our specifications. The robot consists of two 2D Cartesian motion stages arranged in a parallel configuration (Fig. 2). The xy stage provides planar motion relative to the mounting posts, in the plane that corresponds to the face of the template. The workspace of ±4 cm in each direction is sufficient to cover the prostate with a generous margin. The αβ stage rides on the xy stage, with a workspace of ±2 cm. The xy and αβ stages hold a pair of carbon fiber fingers that are manually locked into place during setup. A passive needle guide sleeve is attached between the fingers using free-moving ball joints. We decided against active needle driving. Instead, the robot functions as a fully encoded stable needle guide, through which the physician manually inserts the needle into the patient. The physician thus retains full control and natural haptic sensing, while the needle is being observed in live transverse and sagittal TRUS thus ensuring exquisite control of the insertion depth relative to the target anatomy shown by live ultrasound. If necessary, the insertion depth can also be encoded as in Seidl et al. (2006), thus fully eliminating any practical need for active needle driving.

When the αβ stage is in motion, the guide sleeve performs 2D rotation about the ball joint on the finger attached to the xy stage. The rotational workspace is a ±20° cone, sufficient to provide the required features. The length of the needle guide sleeve was originally 70 mm, providing steady support for the needle against buckling and slipping on the skin. As noted in the Clinical Trial section, the longer guide sleeve made it impossible to access the base of a large prostate; therefore, it was necessary to redesign the fingers to reduce the sleeve length by about 20 mm. Nevertheless, even when using the shorter sleeve for the final three patients, we experienced less needle deflection than a typical brachytherapy procedure. The guide's diameter is slightly above 18G to accommodate standard brachytherapy needles without friction and play. (Note that the sleeve can be made to fit a needle of arbitrary size, such as a biopsy gun.) The sleeve can be snapped in and out of the ball joints by hand and can be disposable. Clinically, it is only necessary to sterilize the fingers and the guide sleeve.

The robot weighs 1300 g. Its dimensions in home position are 140 × 180 × 65 mm. Although it exerts some torque on the template posts, the load is bilaterally distributed over the stepper base with a supporting bracket, a precaution that prevents the robot from bending over the TRUS probe. The bracket is seen in the close-up images of Fig. 5.

The control system architecture is shown in Fig. 3. Low-level robot control is performed on a DMC-2163 controller board and AMP-20341 linear power amplifier (Galil Motion Control, Rocklin, CA, USA), which are connected via Ethernet to the laptop PC that runs the Robot GUI (Graphical User Interface) and the Interplant TPS software processes. Communication between these two processes is provided by a socket (UDP) connection. This required a minor modification to the Interplant software to add a "robot control" menu that invokes a small set of methods, defined in a dynamically loaded library (DLL), to initialize the robot, query its position, and move it to a new position. The DLL transmits these requests, via the socket connection, to the Robot GUI, which then invokes the appropriate methods in the Robot Class. Since the Robot GUI is in a separate process, it can also interact with the user directly; in particular, it updates the robot position/status display and accepts motion commands from the user.

In the current system, the Robot GUI is used to set the needle orientation because these two degrees of freedom are not controlled by the Interplant software. It is also used to move the needle guide to positions that do not lie on the 5 mm template grid. As noted in Fig. 3, most of the custom software created for this project is written in C++ or Python. There is also a safety loop that compares the primary position sensors (incremental encoders) to the secondary position sensors (incremental encoders). This is written

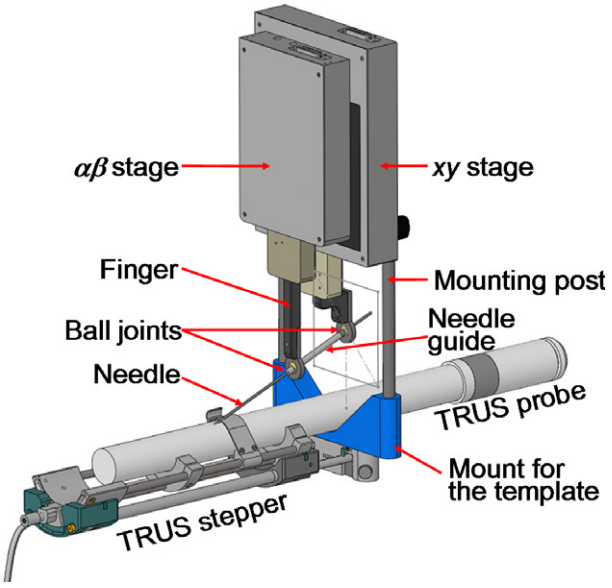

Fig. 2. CAD model of the parallel robot mounted over the TRUS probe on the mounting posts of the template.

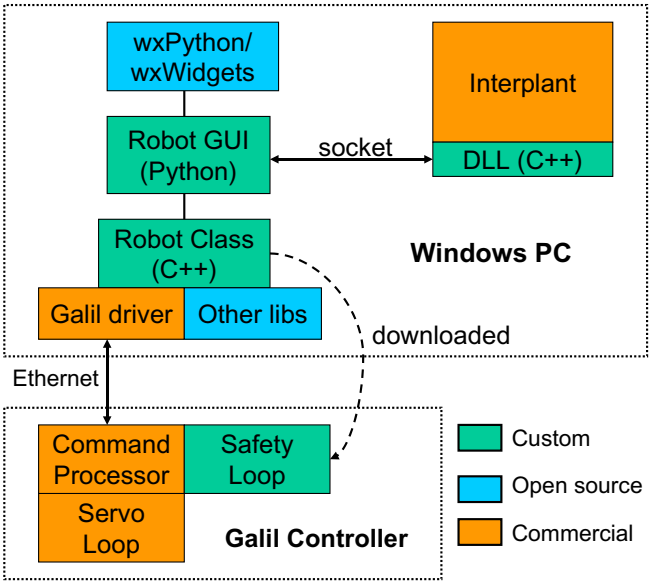

Fig. 3. The robot control architecture.

in a Galil-specific interpreted language and is downloaded to the controller during initialization.

3. Clinical workflow

The calibration of the robot is identical to that of the commercial Interplant® brachytherapy system and uses the same software kit and water tank (Fig. 4.) In essence, we move the needle tip inside the tank in a known trajectory by precise motion of the robot (serving as ground truth) and we also mark the needle positions in sagittal and transverse TRUS images. Then by maximizing the similarity between the observations and the ground truth, we obtain a transformation matrix between the TRUS and robot coordinate frames. As the robot is reliably repositioned on the TRUS stepper in the mounting holes originally made for the template, the robot does not require recalibration before the procedure.

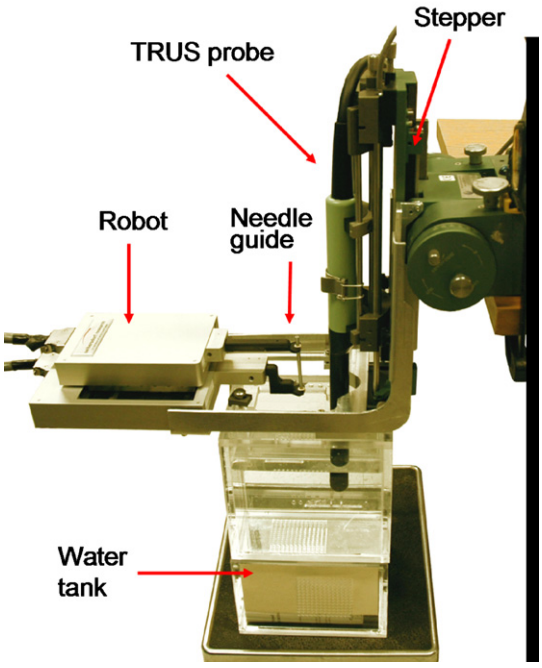

Fig. 4. Calibration with the Interplant kit. Note that the robot replaces the template in an otherwise standard calibration process.

The clinical workflow begins with segmenting the anatomy in TRUS and creating an implant plan. Bilateral stabilization needles may also be inserted. For each implant needle, the coordinates of the desired needle location are sent to the robot. The robot moves the needle guide onto the entry point over the perineum and orients it to the desired angle. The current Interplant dosimetry package does not support slanted needles, but the robot has this functionality. The physician inserts the preloaded needle or seed gun (such as Mick applicator) into the guide sleeve, and enters the needle into the desired depth while observing its progress in the live TRUS. The TPS has a near perfect estimate of the expected location of the needle in TRUS and a visual outline of the planned needle position is superimposed onto the spatially registered TRUS. The TPS semi-automatically processes the image to locate the needle and the operator may apply manual correction. The TPS then can update the dosimetry based upon the inserted needle position. The physician can make manual correction to the needle before approving the position and releasing the payload, or the physician may opt to pull out the needle without releasing the seeds. The physician will retract the needle and release the seeds only after correct needle position is confirmed. During the retraction of the needle, live TRUS images are acquired, wherein shadows of the seeds appear as they are released from the needle. The TPS processes the image to locate the seeds being dropped and the operator may also apply manual correction. Once the seeds are located, the computer promptly calculates a full dosimetry, using the seeds already implanted in their actual delivered locations, combined with the contribution of the remaining planned seeds. At this time, the physician can modify the remainder of the implant plan to compensate for cumulative deviations from the original plan. The cycle of execution is repeated with the next needle until satisfactory dosimetric coverage is achieved, which is the overall objective of the procedure.

4. Phantom studies

We evaluated the prototype system in phantom trials. The robot fits in the neutral space over the perineum (Fig. 1), without obstructing the swing space for a C-arm if one is present. (Later in one clinical case we observed obstruction between the cabling and C-arm.) The robot executed the designed ranges of motions. The Cartesian stage safely covered the axial dimensions of the prostate with generous margin. The function of needle angulation was also tested. Fig. 5(left) depicts sufficient vertical angulation to point the needle behind the pubic arch while Fig. 5(right) demonstrates

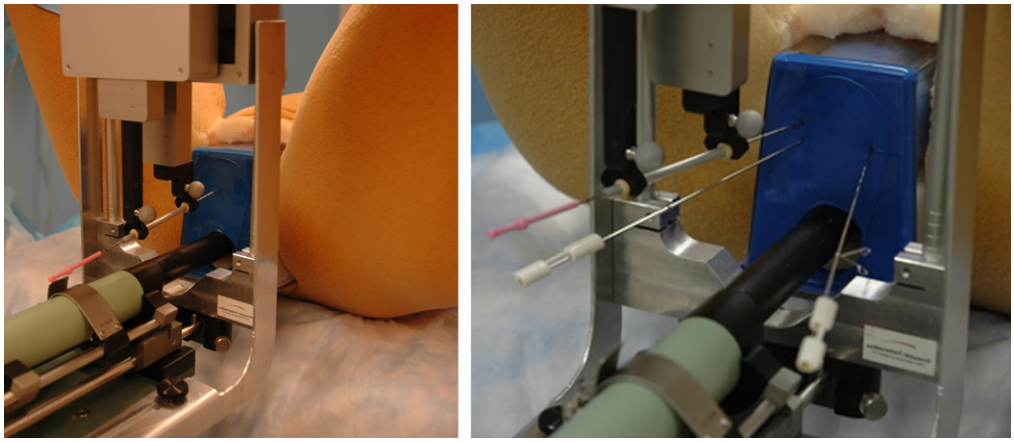

Fig. 5. Insertion of angulated needles. The needle is slanted upward to reach behind the pubic arch (left). Laterally slanted therapy needle in the presence of two stabilizer needles (right).

vertical and lateral angulation. Note that unlike any previous brachytherapy robot system, the implant needles can be inserted in the presence of bilateral stabilizer needles commonly used for reducing prostate motion during needle insertion (Taschereau et al., 2000). In the case of collision, the distal finger gently deflects the stabilizer away, without causing tissue injury, while the physician is standing by to prevent the stabilization needle from being accidentally caught in the robot finger.

We measured the accuracy of robotic needle positioning relative to the template. The robot, as mentioned earlier, is registered to the TRUS and the TPS commands address the robot in template coordinates. We performed 42 parallel positioning movements (7 rows of 6 columns, spaced 1 cm apart) with the robotic system and then manually with the template. We measured the positions of the corresponding template hole and the robotic needle guide before insertion with a calibrated ballpoint pointer (Traxtal Inc., Toronto, ON) tracked by a Polaris tracker (Northern Digital, Waterloo, ON), as seen in Fig. 6(left). The error bars in Fig. 6(middle) show a mean location error of 0.25 mm (STD = 0.17 mm) which is less than the stated accuracy of the tracker. We also measured the accuracy of needle angulation relative to the horizontal axis. We performed 42 robotic positioning movements (7 rows of 6 columns, spaced 1 cm apart, in random angles between the extremes). We measured the angle of the guide sleeve by pivoting on both ends with the calibrated tracker pointer. The error bars shown in Fig. 6(right) display a mean rotation error of 0.75° (STD = 0.37°), comparable with the accuracy of tracking.

We also measured the accuracy of robotic needle positioning followed by needle insertion into the phantom, relative to TRUS. We inserted 18 parallel needles, marked their locations in TRUS and measured the location of the guide sleeve with the Polaris. As shown in Fig. 7, all needles landed close to their goal, with a mean error of 1.04 mm (STD = 0.50 mm). Locations near the prostate edge show somewhat larger errors attributed to slight needle deflection, which is still generously sufficient for brachytherapy. Placement accuracy of slanted needles suggested similar results, but we note that while slanted needles are currently not used in the dose planner, they are useful for adding individual seeds to patch up cold spots.

The apparatus allows for natural haptic feedback, but similarly to current template-based practice, this feeling may be somewhat compromised by friction forces caused by needle bending and sliding forces. Lateral stabilization needles (Taschereau et al., 2000) provide some relief, as Podder et al. (2006) also demonstrated in recent *in vivo* needle force measurements.

In testing the Interplant's capability of producing dynamic dosimetry, standard needles were inserted into a phantom and the moving needle was captured in live TRUS imaged registered in 3D via correlation of the digitally-encoded probe position with

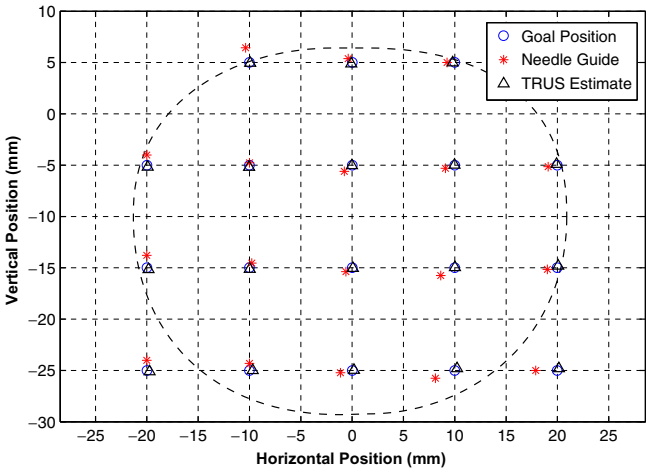

Fig. 7. Accuracy of robotically guided needle insertion relative to target marked in TRUS.

the Interplant stepper and software. A typical screen shot is shown in Fig. 8, where the needle appears in the sagittal image as a white line. The expected seed positions relative to the needle tip are marked with squares. These squares were then used as initial search regions for localizing the seeds upon releasing them into the prostate. The resulting dose display was instantly updated so the clinician could follow the buildup of therapy dose, relative to the anatomy. Color-coded isodose lines seen around the needle are updated as the seeds are captured.

5. Clinical trial

We performed five robot-assisted brachytherapy procedures in an IRB-approved pilot clinical study between August 16, 2007 and November 1, 2007. To our knowledge, to date this has been the only human trial in robotically assisted prostrate brachytherapy. The clinical protocol was to perform the procedure using the standard workflow, except using the robot-held needle guide instead of the template. (We also did not use the dynamic dose optimization option of the TPS, for that function is not directly related to robotic needle placement.) The typical clinical setup is shown in Fig. 9. For the first three cases, we used an optical tracking system (Polaris, Northern Digital Inc.) to verify the needle guide position. This was an optional part of the protocol because the robot already provides redundant position measurement via two encoders on each axis. Nevertheless, the optical tracking system provided an extra level of assurance for the first three cases, to ensure that the needle guide is correctly moved to position by the robot relative to the ori-

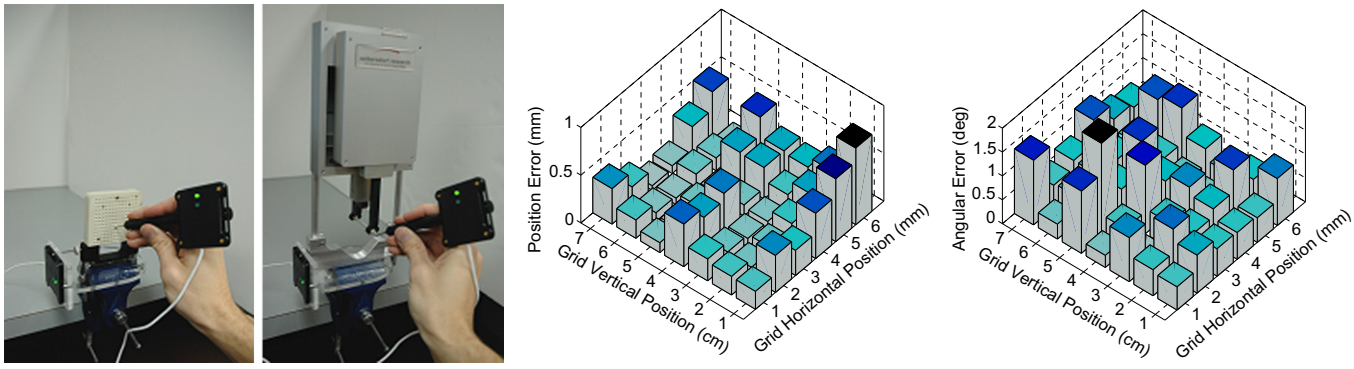

Fig. 6. Comparison of needle guidance between template and robot with Polaris tracker (left). Error bars for the translation (middle) and rotation (right) differences.

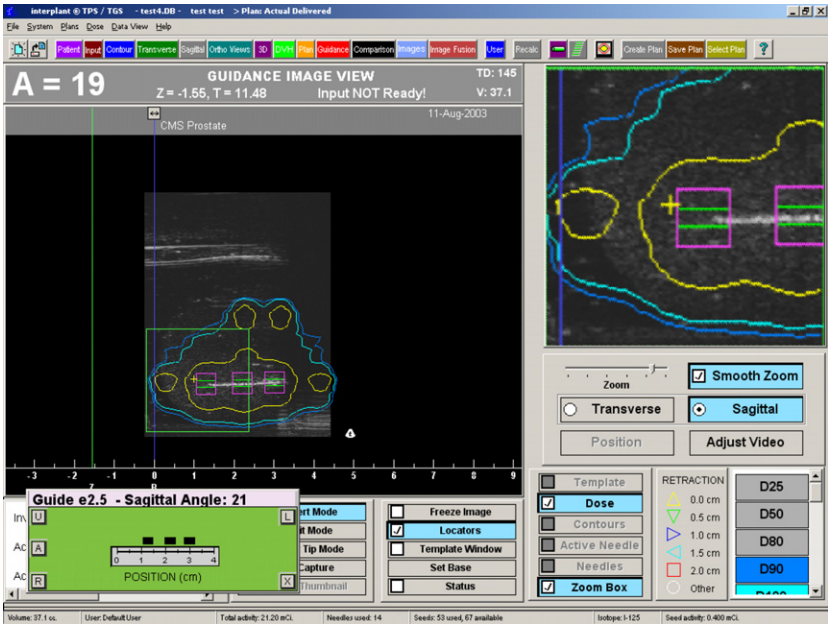

Fig. 8. Dynamic dosimetry screen from Interplant. The needle and seeds are captured in TRUS images as they are being inserted, while the resulting dose display is updated.

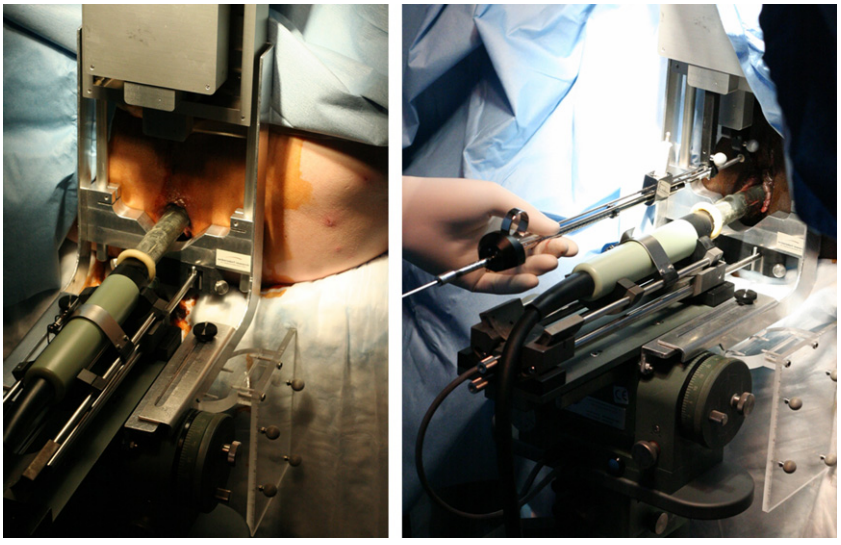

Fig. 9. (Left) Clinical case during setup. The TRUS probe and robot are in place before the robot fingers and needle guide sleeve are attached. (Right) Seed implantation with a Mick applicator.

ginal template coordinate system. We eliminated it for the last two cases because it was difficult to set up due to its requirement for a clear line-of-sight to the marker frames attached to the needle guide and ultrasound stepper. The robot system was successfully used in all five cases. In the first case, it was necessary to revert to the template to place seeds at the base of the prostate because the robot fingers did not allow sufficient depth of needle insertion. Specifically, the hub of the Mick needle (20 cm length) was blocked by the needle guide prior to reaching the prostate base. This problem did not occur in the second case, which was performed immediately after the first one, because the patient's prostate was relatively small. We subsequently modified the fingers to allow an extra 20 mm of needle insertion and this problem did not recur during the final three cases, even though some of the prostates were larger.

Table 1 indicates the total number of needle insertions performed with the robot, and as well as the number of times that the needle guide was adjusted to correct the needle position with respect to the plan (e.g., to compensate for needle deflection) or to make intra-operative modifications to the plan (e.g., to avoid major vessels or the pubic arch). In addition to these temporary adjustments, each of which affects just a single needle, the software also enables adjustment of the robot "home" position. The "home adjustment" shifts the robot coordinate system with respect to the ultrasound image. This was generally done at the start of each procedure to compensate for systematic errors that may remain in the system even after the most careful pre-procedural calibration. In fact, one notable benefit of the robotic system is the ability to easily recalibrate the "template", thereby allowing easy recovery in the occasional situation where there appears to be a systematic error in needle placement despite pre-clinical calibration. (Usually, there is no need to recalibrate the robot to TRUS before the procedure and medical physicists periodically recalibrate TRUS-guided implant systems to detect any mechanical damage or unexpected misalignment.)

Table 1
Number of needle insertions and adjustments for the five patients treated

	#1	#2	#3	#4	#5	Total
Prostate volume (cm^3)	31.1	19.2	28.4	48.2	42.9	
Total needles inserted	35	33	44	31	41	184
Total planned needles	35	31	41	30	38	175
Inserted by robot	30	33	44	31	41	179
Inserted manually	5	0	0	0	0	5
Adjustments to calibration (home adjust)	1	3	2	1	1	8
Adjustments to correct needle position	0	12	12	12	14	50
>2 mm in X	0	5	2	7	6	20
>2 mm in Y	0	2	3	2	1	8
>4 mm in X	0	0	0	1	0	1
>4 mm in Y	0	0	0	0	0	0
Adjustments to modify plan	4	0	9	6	8	27
>2 mm in X	0	0	5	3	5	13
>2 mm in Y	3	0	4	1	2	10
>4 mm in X	0	0	3	0	2	5
>4 mm in Y	1	0	1	0	2	4

The ability to adjust the needle position in small increments was a key feature of the system. It enabled us to make fine adjustments in needle/seed positioning, which we used at times to achieve insertion points between the standard template positions. We found this to be particularly useful toward the end of the procedure if real-time ultrasound dosimetry revealed gaps of dose where one or two precisely placed seeds were needed. In addition, we used this feature to correct for deviations in needle position or to make intraoperative plan modifications, as shown in Table 1 and described above.

The process of needle guide adjustment required the medical physicist to switch between the TPS window and the Robot Control window. For the first three cases, the medical physicist had to manually enter the desired offsets in text windows. This was time consuming and therefore the software was modified prior to the fourth case to add "arrow controls" to the graphical user interface. This change greatly improved the efficiency of the procedure. Future improvements will include an input device to enable direct physician control of the needle guide.

There were some minor issues discovered during the clinical trial. First, we learned that the robotic arms and needle tube had the potential to collide with the ultrasound probe if moved across the center of the prostate along the posterior-most grid row. The order of needle placement was subsequently modified to avoid moving laterally across this area and no further collisions were encountered. Second, the cables that connected to the top of the robot interfered with the normal position of the C-arm fluoroscope. We compensated by introducing a slight gantry tilt of the fluoroscope. This did not affect adversely our ability to obtain the necessary X-ray images during the procedure.

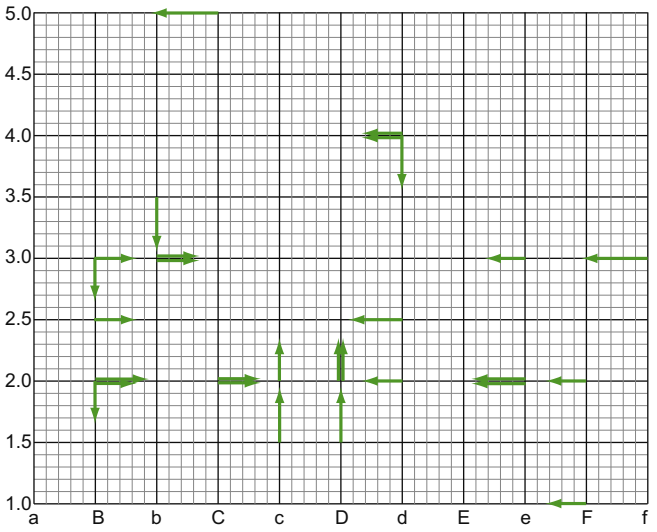

Fig. 10. Direction and magnitude of corrective adjustments ($\geqslant$3 mm) made to the needle position for all five patients. Note the pattern of needles requiring correction toward the center of the prostate, consistent with a tendency for tissue deflection toward the edges of the prostate.

6. Discussion and conclusions

Although our clinical experience is far too small to draw any statistically valid conclusions as to the impact of the robotic template on dosimetric outcomes or toxicity, we have made several observations to its value.

Overall, a relatively small fraction of needle positions required adjustments to be made, and we interpret these adjustments as being required due to tissue deflection of the needle rather than error of robotic positioning. Examination of the direction of the corrective adjustments made (Fig. 10) reveals an overwhelming pattern of needles requiring correction toward the center of the prostate. Needles that miss the target location are usually the ones that are being entered into the periphery of the prostate. When a peripheral needle reaches the slanted prostate capsule, it may skip a little and the prostate may also rotate a bit. The combined result is an apparent outward deflection of the needle. This pattern is consistent with our clinical experience with manual template guidance. In contrast to actual needle tip positions, the Polaris measurements consistently showed the robotic positioning of the needle guide to be accurate generally to within 1mm. Given that the Polaris measurements were of the robot arm position instead of needle position at depth, they are not affected by tissue deflection of the needle upon insertion and thus are a more relevant indication of robotic positioning accuracy versus the template. Actually, we discontinued use of the Polaris after the first three cases due to the effort and room space required for setup and the complete absence of clinically relevant error in the measurements of 112 consecutive needle insertions.

The robot allowed for fine adjustments in needle/seed positioning, which we used at times to achieve insertion points between the standard template positions. In addition, the ability to easily shift the frame of reference of the robotic needle guide avoids a difficult situation encountered in standard procedures where systematic errors in needle placement are often observed despite careful pre-clinical calibration. In such cases, we could easily compensate

for the apparent bias by moving the frame of reference by a few millimeters. This function is not easily possible with standard templates, where the physicist must manually override the results of system calibration, which is not advisable practice from an operational safety perspective. (It may actually constitute as unspecified use of an FDA-approved product, unless the TPS manual specifically allows for such override.)

It also attests to the general safety of our system that the robotic assistance in patient #1 (when the base of his large prostate could not be reached) could be aborted in a matter of minutes and the procedure was concluded with manual template guidance, without noticeable interruption of the workflow. This was made possible by the conscious design decision to maintain a common frame of reference for the robot and the conventional manual template.

It is of particular note that we encountered only a few positioning errors of a magnitude greater than 4 mm, in 2 of 179 needles inserted with the robot, in contrast to our experience with a traditional template guidance where errors of this magnitude are much more common. This could be due to the greater length of the needle guidance tube as compared to the depth of a standard template, allowing for less needle bending outside the tissues. This, if confirmed by follow-up studies, can have a positive impact on clinical outcome. First, needle adjustments increase the number of needle passes and tissue trauma, with resultant exacerbation of urinary symptoms (Eapen et al., 2004; Brammer et al., 2007). Hence fewer adjustments should contribute to a mitigation of severe urinary side effects. Second, reducing the number of needle re-insertions and adjustments should lessen the probability of severe edema. Despite all precautions and strict control of the workflow, intraoperative edemas still cause significant dosimetric uncertainties, which is an issue under intense clinical investigation by several luminaries of prostate brachytherapy. After faulty source placement, edema is arguably the second most significant cause of failure in localized prostate therapies (Yamada et al., 2003). Generally speaking, cancerous tissues receive proportionally less dosage as more edematic fluid accumulates in the prostate. Our recent intraoperative data reveal that edema occurs immediately after needle placement begins and continues to evolve during the procedure (Jain et al., 2007). Edema typically subsides after 2–4 weeks, however by then much of the dose is already delivered due to the short half-life of the isotopes (Pd^{103} = 17 days, I^{125} = 60 days). Although edema results in a ~30% increase in prostate size when evaluated at Day 1 post-implantation, the degree of edema varies substantially from patient to patient with no apparent predictive factors for its magnitude or effects on implant dosimetry (Tanaka et al., 2007). It is therefore absolutely imperative that the probability of edema be reduced, by reducing the number of needle passes and adjustments, and also by shortening the duration of the implant procedure.

The last line in Table 1 shows procedure time, from the first to the last needle, as recorded in the TPS. The average implant time was 1:02 h, which corresponds to an average of about 1:42 min per needle, including TRUS and fluoroscopy confirmation. In the first patient, we lost 16 min because the Mick applicator fell on the floor and had to be re-sterilized, plus the robot had to be dismounted before the last five needles as we mentioned earlier. Not counting the lost 16 min, the average procedure and needle times were 0:59 h and 1:37 min, respectively. The use of the robotic assistant did not slow down the procedure, which must be considered as a very positive result for a pilot clinical trial. We further note that motorized source loading and automated needle insertion could not make our procedure much faster, because we already use a semi-automatic Mick 200-TPV applicator gun.

In addition to the observed benefits described above, robotic needle positioning offers potential for more conformal treatment planning due to the capability for finer adjustments in needle positioning, as well as the potential for reduced number of needles required for a given volume. Again, confirmation and/or measurement of the magnitude of these effects require further investigation. The current robotic system also supports many types of sources and needles. For example, Fig. 5 shows a solo needle loaded with loose seeds and Fig. 9(right) shows a Mick 200-TPV applicator gun. The robotic assistant can be used with both pre-planned and intraoperative dosimetry techniques (Wallner et al., 2001). The device can also function in the presence of stabilizer needles inserted in the prostate before inserting therapy needles, as seen in Fig. 5(right). This feature makes the system potentially usable with real-time inverse dosimetry planning, where a plurality of needles are inserted prior to optimizing the seed loading plan based on actual needle positions (Acher et al., 2006). To utilize inverse optimization, however, software modifications in the TPS will be necessary. Future plans also include testing of the angulation function of the robotic template, which we did not perform in this study; this function also requires modification to the TPS, which is currently underway. Here, we must acknowledge the benefits of having access to the internals of a commercial TPS. This capability allows us to meet clinical needs on the fly, as they arise during the research process, while remaining in the comfort zone of a familiar, well-tested, clinically certified system. This clearly is a unique advantage to our research program.

Further development of the robotic assistant includes motorizing the TRUS base which already performs optical encoding of the stepper, making such a process relatively straightforward. Note that the current system is functional without such motorization of the TRUS probe, though it requires some degree of manual adjustment during needle insertion and seed release, which from the dosimetric point of view is an issue of convenience. A fully integrated digitally-encoded system allows for synchronized imaging and image-based needle/seed tracking, thus opening the way for online dosimetry and instantaneous implant optimization. Work continues to implement advanced automated needle and seed localization techniques, along the lines of excellent prior work by Fenster and his colleagues (Ding et al., 2006; Wei et al., 2006). We also plan modifications of the robot control interface to allow the physician to control the robot rather than communicating verbally with the physicist sitting aside the field of action. Software prediction and avoidance of collisions with the ultrasound probe will be a must from the perspective of operation safety.

As we explained in Section 2, in the current embodiment we opted against active needle driving. We felt that motorized needle insertion would cause the loss of natural haptic sensing, increase the complexity of hardware and invoke a range of extra safety measures. Although these negative factors today outweigh potential benefits, the balance might tip in the future. Phantom tests with robotic "drilling" promise reduced needle deflection and deformation/dislocation of the target tissue (Meltsner et al., 2007). Several groups are experimenting with needle steering. Okamura's group (Webster et al., 2006; Kallem and Cowan, 2007) and Riviere's group (Engh et al., 2006) reported on successful steering of super-elastic beveled needles in soft tissues, by controlled simultaneous spinning and advancing of the needle. They achieved complex insertion trajectories in gel phantoms. Less intricate paths are sufficient for prostate implants, which they could possibly achieve with more rigid needles suitable for transperineal penetration. DiMaio and Salcudean (2005) and Glozman and Shoham (2006) were successful in steering flexible needles in gel phantoms by manipulating the base of the needle driver. Salcudean's group (Okazawa et al., 2005) reported on a hand-held device to steer relatively rigid needles by using telescopic shape memory alloy cannulas. This approach is particularly promising for prostate implants

to achieve slight trajectory corrections upon penetrating the perineal wall and the prostate capsule. With our robotic system, needle steering may be achieved by changing the angle of the needle guide during insertion. Several groups, including Alterovitz et al. (2005) and Goksel et al. (2006), are developing predictive biomechanical models for intraprostatic needle placement. It is safe to predict that predictive models will be coupled with active needle steering in the near future. Clearly, there has been a wealth of exciting research underway that will undoubtedly shape the role of robotic assistance in prostate brachytherapy.

In conclusion, our early experience with the robotic assistant system has been positive. The system provided needle placement accuracy superior to that of conventional templates while offering much greater flexibility, owing to its biaxial needle angulation and continuum Cartesian needle spacing. These features were achieved without causing interference with established clinical hardware, workflow, or calibration standards. This is especially important as commercial potential and clinical viability in contemporary medicine are inseparable issues. Although these benefits appeared to be clearly demonstrated in our limited clinical trial, it is necessary to confirm them in larger and statistically more significant studies.

Acknowledgements

We are grateful to Theodore L. DeWeese, MD, for clinical guidance; to Elwood Armour, PhD, and Yi Lee, PhD, for medical physics support; to Anton Deguet, MSc, for technical assistance during the clinical trials; to Wolfgang Ptacek, MSc; for mechanical design; to Jack Blevins, BS, for software modifications in the Interplant® treatment planning system; to Daryl Carson, BS, for managing regulatory issues. This project could not have been possible without their unrelenting help and dedication. Our program has been financially supported by the US government, through DoD PC-050042, DoD PC050170, NIH 5R44 CA088139, NIH 1R41 CA106152, and the NSF Engineering Research Center for Computer Integrated Surgical Systems and Technology under EEC-9731748.

References

Acher, P., Popert, R., Nichol, J., Potters, L., Morris, S., Beaney, R., 2006. Permanent prostate brachytherapy: dosimetric results and analysis of a learning curve with a dynamic dose-feedback technique. Int. J. Radiat. Oncol. Biol. Phys. 65 (3), 694–698.

Alterovitz, R., Goldberg, K., Okamura, A., 2005. Planning for steerable bevel-tip needle insertion through 2D soft tissue with obstacles. In: IEEE International Conference on Robotics and Automation (ICRA), pp. 1652–1657.

Brammer, S., Merrick, G.S., Butler, W., et al., 2007. The impact of needle trauma on urinary, bowel, and erectile function following transperineal template guided prostate saturation biopsy: implications for brachytherapy. Int. J. Radiat. Oncol. Biol. Phys. 69 (Suppl. 3), S350.

Cooperberg, M.R., Broering, J.M., Litwin, M.S., et al., 2004. The contemporary management of prostate cancer in the United States: lessons from the cancer of the prostate strategic urologic research endeavor (CapSURE), a national disease registry. J. Urol. 171 (4), 1393–1401.

DiMaio, S.P., Salcudean, S.E., 2005. Interactive simulation of needle insertion models. IEEE Trans. Biomed. Eng. 52 (7), 1167–1179.

Ding, M., Wei, Z., Gardi, L., Downey, D.B., Fenster, A., 2006. Needle and seed segmentation in intra-operative 3D ultrasound-guided prostate brachytherapy. Ultrasonics 44 (Suppl. 1), e331–e336.

Eapen, L. et al., 2004. Correlating the degree of needle trauma during prostate brachytherapy and the development of acute urinary toxicity. Int. J. Radiat. Oncol. Biol. Phys. 59 (5), 1392–1394.

Engh, J.A., Podnar, G., Khoo, S., Riviere, C., 2006. Flexible needle steering system for percutaneous access to deep zones of the brain. In: Proceedings of the IEEE 32nd Annual Northeast Bioengineering Conference, pp. 103–104.

Fichtinger, G., DeWeese, T.L., Patriciu, A., et al., 2002. Robotically assisted prostate biopsy and therapy with intra-operative CT guidance. J. Acad. Radiol. 9 (1), 60–74.

Fichtinger, G., Burdette, E.C., Tanacs, A., et al., 2006. Robotically assisted prostate brachytherapy with transrectal ultrasound guidance–Phantom experiments. Brachytherapy 5 (1), 14–26.

Fichtinger, G., Fiene, J., Kennedy, C., Iordachita, I., Kronreif, G., Song, D.Y., Burdette, E.C., Kazanzides, P., 2007. Robotic assistance for ultrasound guided prostate brachytherapy. In: Tenth International Conference on Medical Image Computing and Computer-Assisted Intervention (MICCAI). Lecture Notes in Computer Science, vol. 4791, pp. 119–127.

Glozman, D., Shoham, M., 2006. Flexible needle steering for percutaneous therapies. Comp. Aid. Surg. 11 (4), 194–201.

Goksel, O., Salcudean, S.E., DiMaio, S.P., 2006. 3D simulation of needle–tissue interaction with application to prostate brachytherapy. Comp. Aid. Surg. 11 (6), 279–288.

Harmat, A., Rohling, R., Salcudean, S., 2006. Needle tip localization using stylet vibration. Ultrasound Med. Biol. 32 (9), 1339–1348.

Harris, S.J., Arambula-Cosio, F., Mei, Q., Hibberd, R.D., Davies, B.L., Wickham, J.E., Nathan, M.S., Kundu, B., 1997. The Probot—an active robot for prostate resection. Proc. Inst. Mech. Eng. [H]. 211 (4), 317–325.

Jain, A.K., Deguet, A., Iordachita, I., Chintalapani, G., Blevins, J., Le, Y., Armour, E., Burdette, C., Song, D., Fichtinger, G., 2007. Intra-operative guidance in prostate brachytherapy using an average C-arm. In: Tenth International Conference on Medical Image Computing and Computer-Assisted Intervention (MICCAI), Lecture Notes in Computer Science, vol. 4792, pp. 9–16.

Jemal, A., Siegel, R., Ward, E., Murray, T., Xu, J., Smigal, C., Thun, M.J., 2006. Cancer statistics 2006. CA Cancer J. Clin. 56 (2), 106–130.

Kallem, V., Cowan, N.J., 2007. Image-guided control of flexible bevel-tip needles. In: IEEE International Conference on Robotics and Automation (ICRA), Rome, Italy, pp. 3015–3020.

Kettenbach, J., Kronreif, G., Figl, M., et al., 2005. Robot-assisted biopsy using ultrasound guidance: initial results from in vitro tests. Eur. Radiol. 15, 765–771.

Masamune, K., Fichtinger, G., Patriciu, A., Susil, R.C., Taylor, R.H., Kavoussi, L.R., Anderson, J.H., Sakuma, I., Dohi, T., Stoianovici, D., 2001. System for robotically assisted percutaneous procedures with computed tomography guidance. J. Comp. Aid. Surg. 6 (6), 370–383.

Meltsner, M.A., Ferrier, N.J., Thomadsen, B.R., 2007. Observations on rotating needle insertions using a brachytherapy robot. Phys. Med. Biol. 52 (19), 6027–6037.

Merrick, G.S., Butler, W.M., Wallner, K.E., et al., 2003. Rectal function following brachytherapy with or without supplemental external beam radiation: results of two prospective randomized trials. Brachytherapy 2, 147–157.

Merrick, G.S., Grimm, P.D., Sylvester, J., Blasko, J.C., Butler, W.M., Allen, Z.A., Chaudhry, U.U., Mazza, A., Sitter, M., 2007. Initial analysis of Pro-Qura: a multi-institutional database of prostate brachytherapy dosimetry. Brachytherapy 6 (1), 9–15.

Miller, D.C., Sanda, M.G., Dunn, R.L., Montie, J.E., Pimentel, H., Sandler, H.M., et al., 2005. Long-term outcomes among localized prostate cancer survivors: health-related quality-of-life changes after radical prostatectomy, external radiation, and brachytherapy. J. Clin. Oncol. 23, 2772.

Nag, S., Ciezki, J.P., Cormack, R., et al., 2001. Intraoperative planning and evaluation of permanent prostate brachytherapy: report of the American brachytherapy society. Int. J. Radiat. Oncol. Biol. Phys. 51, 1420–1430.

Okazawa, S., Ebrahimi, R., Chuang, J., Rohling, R., Salcudean, S.E., 2005. Hand-held Steerable Needle Device. IEEE/ASME Trans. Mechatronics 10 (3), 285–296.

Okazawa, S., Ebrahimi, R., Chuang, J., Rohling, R., Salcudean, S.E., 2006. Methods for segmenting curved needles and the needle tip in real-time ultrasound imaging. Med. Image Anal. 10 (3), 330–342.

Patriciu, A., Petrisor, D., Muntener, M., Mazilu, D., Schär, M., Stoianovici, D., 2007. Automatic brachytherapy seed placement under MRI guidance. IEEE Trans. Biomed. Eng. 54 (8), 1499–1506.

Phee, L., Yuen, J., Xiao, D., et al., 2006. Ultrasound guided robotic biopsy of the prostate. Int. J. Human. Robot. 3 (4), 463–483.

Podder, T., Clark, D., Sherman, J., Fuller, D., Messing, E., Rubens, D., Strang, J., Brasacchio, R., Liao, L., Ng, W.S., Yu, Y., 2006. In Vivo motion and force measurement of surgical needle intervention during prostate brachytherapy. Med. Phys. 33 (8), 2915–2922.

Seidl, K., Fichtinger, G., Kazanzides, P., 2006. Optical Measurement of Needle Insertion Depth. IEEE International Conference on Biomedical Robotics (BioRob), Pisa, Italy, pp. 799–804.

Tanaka, O., Hayashi, S., Matsuo, M., et al., 2007. Effect of edema on postimplant dosimetry in prostate brachytherapy using CT/MRI fusion. Int. J. Radiat. Oncol. Biol. Phys. 69, 614–618.

Taschereau, R., Pouliot, J., Roy, J., et al., 2000. Seed misplacement and stabilizing needles in transperineal permanent prostate implants. Radiother. Oncol. 55, 59–63.

Wallner, K., Blasko, J.C., Dattoli, M., 2001. Prostate Brachytherapy made Complicated, second ed. SmartMedicine Press, Seattle, WA.

Wan, G., Wei, Z., Gardi, L., et al., 2005. Brachytherapy needle deflection evaluation and correction. Med. Phys. 32, 902–909.

Webster III, R.J., Kim, R.J., Cowan, N.J., Chirikjian, G.S., Okamura, A.M., 2006. Nonholonomic modeling of needle steering. Int. J. Robot. Res. 25 (5–6), 509–525.

Wei, J.T., Dunn, R.L., Sandler, H.M., McLaughlin, P.W., Montie, J.E., Litwin, M.S., Nyquist, L., Sanda, M.G., 2002. Comprehensive comparison of health-related quality of life after contemporary therapies for localized prostate cancer. J. Clin. Oncol. 20 (2), 557–566.

Wei, Z., Wan, G., Gardi, L., et al., 2004. Robot-assisted 3D-TRUS guided prostate brachytherapy: system integration and validation. Med. Phys. 31 (3), 539–548.

Wei, Z., Gardi, L., Downey, D.B., Fenster, A., 2006. Automated localization of implanted seeds in 3D TRUS images used for prostate brachytherapy. Med. Phys. 33 (7), 2404–2417.

Yamada, Y., Potters, L., Zaider, M., Cohen, G., Venkatraman, E., Zelefsky, M.J., 2003. Impact of intraoperative edema during transperineal permanent prostate

brachytherapy on computer-optimized and preimplant planning techniques. Am. J. Clin. Oncol. 26 (5), e130–e135.

Yu, Y., Podder, T.K., Zhang, Y.D., Ng, W.S., Misic, V., Sherman, J., Fuller, D., Rubens, D.J., Strang, J.G., Brasacchio, R.A., Messing, E.M., 2007. Robotic system for prostate brachytherapy. Comp. Aid. Surg. 12 (6), 366–370.

Zelefsky, M.J., Yamada, Y., Cohen, G., et al., 2000. Postimplantation dosimetric analysis of permanent transperineal prostate implantation: Improved dose distribution with an intraoperative computer-optimized conformal planning technique. Int. J. Radiat. Oncol. Biol. Phys. 48, 601–608.

Zelefsky, M.J., Yamada, Y., Marion, C., et al., 2003. Improved conformality and decreased toxicity with intraoperative computer-optimized transperineal ultrasound-guided prostate brachytherapy. Int. J. Radiat. Oncol. Biol. Phys. 55, 956–963.